

## CRYSTAL SIZE AND ORIENTATION PATTERNS IN THE WISCONSIN-AGE ICE FROM DYE 3, GREENLAND

by

C.C. Langway, Jr, H. Shoji and N. Azuma

(Department of Geological Sciences, State University of New York at Buffalo,  
4240 Ridge Lea Road, Amherst, NY 14226, U.S.A.)

### ABSTRACT

Crystal size and *c*-axis orientation patterns were measured on the Dye 3, Greenland, deep ice core in order to investigate time-dependent changes or alterations in the physical character of the core as a function of time after recovery. The physical measurements were expanded to include depth intervals not previously studied in the field. The recent study focused on core samples located between 1786 m and the bottom of the ice sheet at 2037 m.

Manual *c*-axis measurements were made on 23 new thin sections using a Rigsby-type universal stage. A new semi-automatic ultrasonic wave-velocity measuring device was developed in order to compare the results with the earlier manual measurements and to study an additional 114 ice-core samples in the Wisconsin-age ice. Crystal-size measurements were made on specimen surfaces by inducing evaporation grooves at crystal boundaries and measuring linear intercepts. The ultrasonically measured test samples were subsequently cleaned and analyzed by ion chromatography in order to measure impurity concentration levels of  $\text{Cl}^-$ ,  $\text{NO}_3^-$  and  $\text{SO}_4^{2-}$  and study their effects on crystal growth and *c*-axis orientation.

### INTRODUCTION

To understand the dynamic processes which occur within the mass of a polar glacier it is necessary to measure the physical-property variations over the vertical profile. A continuous 2037 m long Greenland Ice Sheet Program (GISP) core ice was recovered at Dye 3, Greenland (65°11'N, 43°49'W) between 1979 and 1981 (Gundestrup and Johnsen 1985, Langway and others 1985); it provided glacier-ice samples from the surface to bedrock of excellent quality for such an investigation. Initial multi-parameter physical measurements were made on the Dye 3 core in a field-trench laboratory immediately after each core section was augered (S.L. Herron and others 1985). Other physical-property studies were made after the ice core had been transported back to the laboratory (Shoji and Langway 1982 and 1983, S.L. Herron and Langway unpublished, Azuma unpublished).

The Holocene-Wisconsin boundary for the Dye 3, Greenland, ice core was identified at 1786 m depth by the stable-isotope method (Dansgaard and others 1982 and 1985) and confirmed by simultaneous sharp changes in measurements of the physical properties and an increase in wave velocity (S.L. Herron and others 1985), by a pronounced increase in  $\text{Cl}^-$ ,  $\text{NO}_3^-$  and  $\text{SO}_4^{2-}$  concentration levels (M.M. Herron and Langway 1985), by a lower conductivity and a higher dust content (Hammer and others 1985), and by a higher strain-rate enhancement factor (Shoji and Langway 1985).

The laboratory studies presented here focus on core samples from the Wisconsin-age ice located between the 1786 m depth and the bottom of the ice sheet. Manual *c*-axis crystal-orientation measurements were made on 23 new thin sections using a Rigsby-type universal stage. A new semi-automatic crystal-orientation technique which makes use of ultrasonic wave velocities was used to measure *c*-axes on 114 other core samples. Crystal-size measurements

were made on both sets of specimens. The ultrasonically measured test samples were subsequently cleaned and prepared for chemical analyses by ion chromatography in order to study the effect of impurity concentrations on the physical parameters. The results of core studies on the air bubbles, air hydrates, megascopic stratigraphy, melt layers, porosity and air permeability, micro-hardness and crystal anisotropy in the upper firn structure of the Dye 3 deep ice core will be reported elsewhere.

### SAMPLES AND METHODS

Manual crystal orientations were made on the 23 thin sections, applying procedures outlined by Langway (1958), using a Rigsby-type universal stage. Crystal size was measured directly on the thin sections or from enlarged photographs. The sections were cut perpendicular to the long ice-core axis. No azimuth control was obtained.

The core samples for ultrasonic wave-velocity measurements were prepared from 3.5 cm thick vertical sections cut parallel to the long axis of the ice core. Each vertical rectangular block section (8 × 8 × 3.5 cm) was first cut by band saw and then smooth-finished, using a microtome blade. No azimuth control was obtained. All samples were systematically spaced at an interval of about

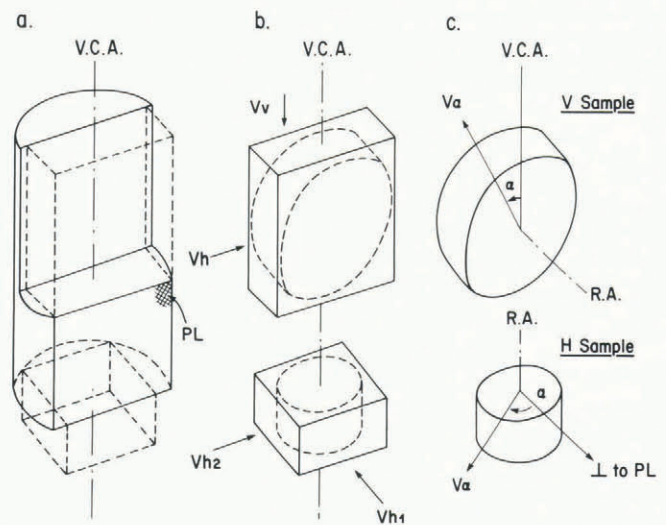


Fig. 1. Sample-preparation procedures for ultrasonic wave-velocity measurements. The vertical specimen (upper figures) and horizontal specimen (lower figures) are both part of the same ice-core sample. (a) Specimens are cut parallel (PL) to the long vertical core axis (V.C.A.). (b) After ultrasonic velocity measurements, each specimen is lathed into cylinders. (c) Ultrasonic velocity is measured along the circumference of the cylinder on a rotation axis (R.A.) which is perpendicular to PL (vertical specimen) or parallel to V.C.A. (horizontal specimen).

TABLE I. THIN-SECTION SAMPLES FROM THE WISCONSIN-AGE DYE 3 ICE CORE.

Sample no.	Depth m	Number of <i>c</i> -axes measured (N)	Fabric statistics (R/N)	Inclination of mean <i>c</i> -axes from core axis degree	Grain-size mm
1	1658.40	99	0.82	1	>10
2	1820.67	140	0.98	12	0.91
3	1836.45	157	0.95	10	1.2
4	1850.45	150	0.97	11	1.1
5	1852.20	150	0.96	10	0.93
6	1860.22	190	0.95	9	1.7
7	1863.59	200	0.94	8	1.0
8	1867.01	180	0.98	8	1.5
9	1870.89	200	0.94	9	0.92
10	1884.30	178	0.98	9	1.2
11	1889.63	180	0.94	10	1.0
12	1895.27	180	0.98	7	1.7
13	1897.45	132	0.97	8	1.2
14	1899.61	152	0.97	15	1.1
15	1908.27	196	0.97	10	1.9
16	1911.27	184	0.98	9	0.97
17	1929.35	200	0.97	11	2.1
18	1933.24	176	0.94	10	1.4
19	1943.42	132	0.97	5	1.8
20	1961.21	200	0.95	15	1.0
21	1980.11	154	0.98	6	1.8
22	1995.10	188	0.89	10	3.3
23	2006.16	178	0.99	7	2.2

2.2 m within the depth range of 1788 and 2034 m. Sample-preparation and orientation procedures are shown in Figure 1. Ultrasonic wave-velocity measurements were made first on the rectangular blocks in both a vertical ( $V_v$ ) and a horizontal ( $V_h$ ) direction. Thereafter the rectangular block was lathed into a cylindrical shape ( $d = 7$  cm,  $h = 3.5$  cm), as shown in Figure 1. For the new analytical technique the wave velocities were measured along the circumference of the cylinders by mounting the specimen on the lathe carriage and manually rotating the cylinder in increments of  $5^\circ$ . A Krautkramer-Branson USL 38 with a 2.25 MHz transducer was used to propagate an ultrasonic P-wave. A

low-viscosity silicone oil was used as a coupler. Measurements were performed in a  $15^\circ \pm 2^\circ\text{C}$  cold-room. Crystal size was measured on these samples by thermal-etching grain-boundary grooves on the flat surface of the cylinder and measuring linear intercepts. Finally, each sample was surface-microtomed, cleaned and melted, using established clean-room procedures, and measured for  $\text{Cl}^-$ ,  $\text{NO}_3^-$  and  $\text{SO}_4^{2-}$  concentration levels by ion chromatography (Langway and Goto-Azuma 1988, this volume), applying procedures previously reported (M.M. Herron and Langway 1985). Samples from the near-bottom silty ice (below 2008 m depth) were not chemically analyzed.

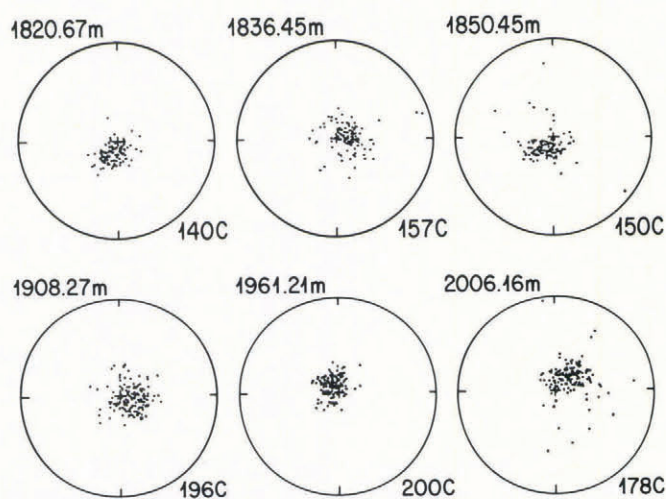


Fig.2. Fabric diagrams of six typical thin sections from Wisconsin-age ice measured on a Rigsby-type stage. The center of each diagram (lower hemisphere of Schmidt-net projection) corresponds to the vertical long-core axis.

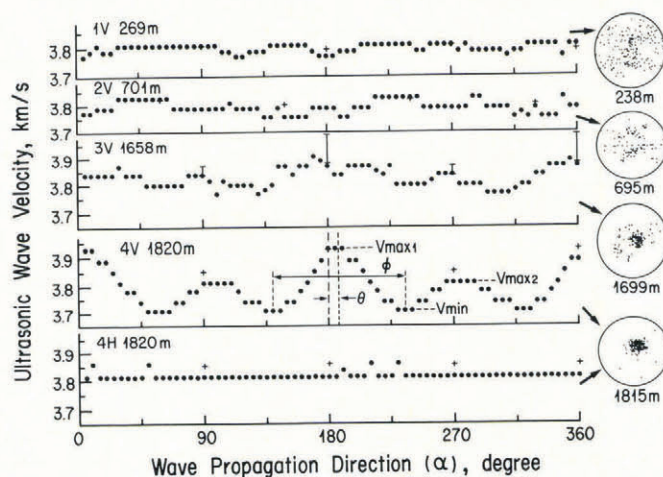


Fig.3. P-wave ultrasonic wave-velocity curves compared with four *c*-axis fabric diagrams measured on a Rigsby-type stage (S.L. Herron and others 1985). Wave propagation is plotted parallel to the vertical plane of the core for vertical specimens (1V, 2V, 3V and 4V) or perpendicular to the long-core axis for the horizontal specimen (4H).

## RESULTS

The results of the fabric and crystal-size measurements on the 23 manually measured sections are listed in Table I. All sections below 1786 m depth show strong single-maximum fabric patterns. As examples, six of the fabric diagrams are shown in Figure 2. Section depth is identified in the top left of each diagram in Figure 2 and the number of crystals measured is shown in the bottom right. The results of these measurements were compared with similar field measurements which were made by S.L. Herron and others (1985) in order to investigate possible time-dependent changes or alterations in the physical character of the ice cores. No marked differences in orientation pattern or changes in grain-size were observed either in the thin sections reported on here or in the sections measured in the field about 5 years earlier.

Previously reported studies of the crystal anisotropy in ice sheets were usually made by measuring the ultrasonic velocities on selected ice-core samples in two directions: the vertical and the horizontal (Bennett 1972, Kohnen and Langway 1977, Kohnen and Bentley 1977). For this study a new semi-automatic multi-directional technique was developed. The feasibility of the method was first tested by comparing the semi-automatic results from the 269, 701, 1658 and 1820 m depths with the field results of S.L. Herron and others (1985) at the 238, 695, 1699 and 1815 m depths respectively (Fig.3). As shown in Figure 3, the ultrasonic wave-velocity curve which results from measuring sample 1V from 269 m is nearly constant throughout the 360° rotation and corresponds quite well to the random orientation pattern indicated in the fabric diagram of the 238 m section. Curve 2V from 701 m shows slightly higher wave velocities between 30° and 65°, which corresponds to the slightly more circular convergence of *c*-axes shown in the fabric diagram at 695 m. The 2V velocity curve is asymmetrical with reference to  $\alpha = 180^\circ$  because the *c*-axis concentration is asymmetrical. Curve 3V from 1658 m shows the highest velocity values to be near vertical and compares favorably with the strong vertical fabric pattern displayed in the diagram from 1669 m. Curve 4V from 1820 m shows a pronounced and relatively smooth sinusoidal velocity curve, which is reflected as a very strong, near-vertical, single-maximum fabric pattern in the diagram from 1815 m. Some velocity curves show a flat-velocity maximum and minimum along the wave-propagation direction due to the  $\pm 8$  m/s velocity resolution limits of the apparatus. Crosses superimposed on the velocity curves in Figure 3 represent velocity measurements made on the 114 block samples in two directions before the cylinder was made and tested. The velocity differences result from the resolution limits of the apparatus and the geometry of the sample. Temperature-induced error in velocity measurements is estimated to be within 10 m/s. Curve 4H from the 1820 m specimen ( $d = 4.5$  cm,  $h = 3.5$  cm) indicates that the wave velocity in the horizontal plane is nearly isotropic, as it should be when wave-propagation direction is constantly oriented perpendicular to a strong vertically oriented fabric pattern. The above study demonstrates the validity of the multi-directional ultrasonic wave-velocity measurements for determining *c*-axis crystal-orientation data over a complete spectrum of fabric patterns and configurations.

Since the pole of a strong single-maximum fabric pattern is coincident to the pole of the mean *c*-axis direction, additional detailed information can be obtained by considering the geometry of the *c*-axis distribution patterns. The ultrasonic velocity should be highest along the pole direction and decrease as the angle increases from the mean pole direction. The lower velocity ( $V_{\min}$ ) directions result in a cone-shaped configuration in which the half-apex angle is approximately 50° (Bennett 1972). The velocity then increases to the second highest velocity ( $V_{\max 2}$ ) as the wave propagation direction is inclined more than 50° from the pole. In this orientation, measurements are made along a direction perpendicular to the pole direction. Since the ice-crystal *c*-axis pole direction is not usually found parallel to the vertical cutting plane of the specimen (PL in Figure 1a), the apparent highest velocity ( $V_{\max 1}$ ) is usually measured along an inclined direction,  $\theta$ , from the vertical core axis in PL plane. When the pole direction rotates away from PL plane,  $V_{\max 1}$  decreases, due to the increase in the inclination angle from the pole direction. With this rotation,

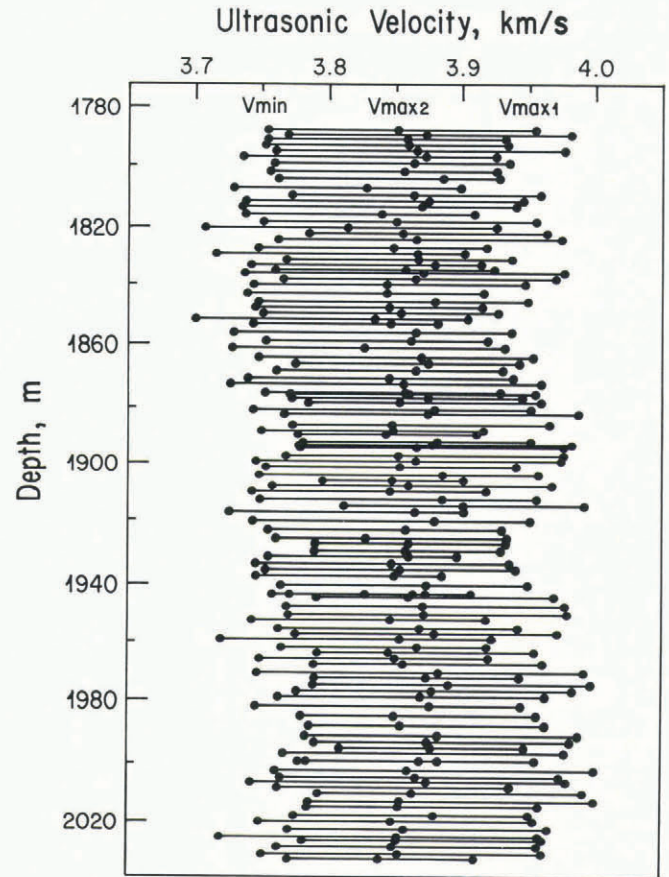


Fig.4. Ultrasonic wave velocities measured on the 114 Wisconsin-age ice specimens. The measured values of  $V_{\max 1}$ ,  $V_{\max 2}$  and  $V_{\min}$  are plotted at each specimen depth. The general feature of data obtained is an approximately constant level of strong anisotropy in *c*-axis orientation distributions for the Wisconsin-age ice, including the bottom silty-ice specimens.

$V_{\max 2}$  and  $V_{\min}$  remain the same, even though the angle distance,  $\phi$ , decreases between two  $V_{\min}$  directions with an interspersed  $V_{\max 1}$ . Therefore,  $\delta V$ , the velocity difference between  $V_{\max 2}$  and  $V_{\min}$ , does not depend on rotation of the pole direction and can be used to indicate the *c*-axis concentration strength along the pole direction.

The results of the semi-automatic ultrasonic wave-velocity measurements on the 114 samples are shown in Figure 4 and listed in Table II. They indicate that a strong single-maximum fabric pattern exists for all Wisconsin-age ice, including the bottom silt-laden ice from below 2008 m depth. With this method it is possible to conduct *c*-axis measurements in core samples which contain embedded debris, where thin sections cannot normally be made for Rigsby-type measurements.

Ice crystal-size data for both the thin-section and ultrasonic-velocity specimens are listed in Tables I and II. Figure 5 shows crystal-size data and  $\text{SO}_4^{2-}$  concentration levels plotted versus depth. Crystal size ranges from 0.5 to 3.0 mm, with considerable variability within these limits. The main trends of the size curve show that larger-sized crystals exist from about 1790 to 1815 m, where a sharp decrease occurs. From about 1815 to 1970 m there is a general and gradual increase in size. Another sharp change to increased size occurs at about 1970 m. At 2005 m the curve again makes a decided shift to much smaller crystal sizes just before the near-bottom silt-laden basal ice appears at about 2008 m. Ice crystals in the silty basal ice are the smallest of the entire profile and average less than 1 mm. Crystal size in the deepest specimen, measured at 2034 m, averaged 0.45 mm.

TABLE II. WAVE-VELOCITY SAMPLES FROM THE WISCONSIN-AGE DYE 3 ICE CORE

Sample no.	Sample depth m	Grain-size mm	$V_{\max 1}$ km/s	$V_{\max 2}$ km/s	$V_{\min}$ km/s	$V(45)$ km/s	Angle ( $\theta$ ) degree	Angle ( $\phi$ ) degree
1	1788.24	2.0	3.955	3.851	3.754	3.769	7.5	98
2	1790.18	0.96	3.982	3.872	3.769	3.785	10	96
3	1791.54	1.1	3.933	3.858	3.754	3.754	5	95
4	1793.43	1.4	3.935	3.859	3.752	3.779	7.5	96
5	1795.43	1.6	3.977	3.865	3.760	3.777	7.5	103
6	1797.43	1.6	3.926	3.872	3.736	3.786	12.5	103
7	1799.43	1.5	3.936	3.863	3.759	3.794	12.5	96
8	1801.94	1.5	3.926	3.856	3.756	3.757	7.5	96
9	1804.42	1.4	3.929	3.885	3.762	3.782	10	99
10	1807.43	1.6	3.899	3.828	3.729	3.752	5	103
11	1809.43	1.6	3.959	3.863	3.772	3.781	2.5	95
12	1811.44	1.5	3.946	3.874	3.738	3.754	7.5	99
13	1813.44	1.1	3.941	3.869	3.735	3.769	10	99
14	1815.94	0.90	3.910	3.839	3.738	3.744	7.5	99
15	1818.44	0.68	3.956	3.850	3.751	3.767	2.5	99
16	1820.44	0.80	3.926	3.814	3.708	3.726	2.5	96
17	1822.44	0.91	3.964	3.855	3.785	3.785	5	101
18	1824.44	0.98	3.975	3.865	3.762	3.759	0	99
19	1827.44	0.82	3.919	3.848	3.747	3.747	2.5	95
20	1829.44	0.81	3.902	3.866	3.716	3.724	2.5	95
21	1831.44	0.85	3.938	3.867	3.768	3.768	12.5	95
22	1833.44	0.90	3.915	3.879	3.742	3.739	2.5	95
23	1835.35	0.80	3.925	3.857	3.760	3.759	5	95
24	1836.35	0.94	3.977	3.870	3.737	3.739	2.5	100
25	1838.41	0.82	3.971	3.865	3.766	3.782	10	100
26	1840.35	0.81	3.948	3.843	3.744	3.759	2.5	101
27	1843.35	0.83	3.917	3.843	3.739	3.773	12.5	100
28	1846.27	0.96	3.950	3.879	3.747	3.781	12.5	94
29	1848.13	0.76	3.916	3.845	3.745	3.745	10	93
30	1850.35	0.94	3.928	3.854	3.751	3.751	7.5	99
31	1852.09	0.63	3.905	3.834	3.701	3.714	7.5	99
32	1853.56	0.64	3.881	3.846	3.744	3.744	5	95
33	1856.35	0.85	3.938	3.865	3.729	3.739	5	94
34	1859.09	1.1	3.920	3.862	3.753	3.770	7.5	103
35	1861.26	0.92	3.933	3.827	3.728	3.749	0	100
36	1864.22	0.92	3.954	3.869	3.748	3.769	0	101
37	1866.27	1.4	3.944	3.874	3.775	3.774	0	100
38	1868.27	0.67	3.931	3.865	3.761	3.771	7.5	99
39	1870.76	0.73	3.939	3.845	3.740	3.749	5	99
40	1872.35	1.3	3.960	3.856	3.727	3.769	7.5	94
41	1875.26	0.97	3.930	3.857	3.753	3.769	12.5	99
42	1875.66	0.85	3.956	3.860	3.771	3.769	5	99
43	1877.08	0.85	3.946	3.874	3.773	3.774	7.5	96
44	1878.54	1.5	3.960	3.853	3.785	3.785	7.5	101
45	1880.85	0.86	3.952	3.879	3.744	3.744	7.5	103
46	1882.43	1.6	3.988	3.874	3.767	3.785	10	103
47	1886.08	1.3	3.966	3.847	3.773	3.792	7.5	100
48	1888.29	0.78	3.917	3.848	3.750	3.759	12.5	99
49	1889.57	0.86	3.912	3.843	3.777	3.774	5	95
50	1892.61	1.3	3.953	3.881	3.781	3.819	20	104
51	1893.55	1.5	3.983	3.877	3.777	3.787	5	101
52	1894.37	1.4	3.977	3.866	3.779	3.779	12.5	100
53	1897.37	2.0	3.977	3.852	3.768	3.799	7.5	91
54	1899.37	0.79	3.975	3.865	3.746	3.779	10	99
55	1901.37	1.1	3.941	3.853	3.753	3.777	10	99
56	1904.37	1.0	3.958	3.885	3.748	3.779	12.5	99
57	1906.39	1.2	3.902	3.848	3.796	3.796	5	103
58	1908.37	1.3	3.968	3.860	3.758	3.759	5	93
59	1910.37	0.99	3.919	3.846	3.743	3.754	7.5	98
60	1913.29	1.4	3.957	3.885	3.749	3.764	7.5	99
61	1915.37	1.8	3.992	3.901	3.812	3.809	5	96
62	1917.38	1.1	3.902	3.865	3.726	3.729	0	96



TABLE II. WAVE-VELOCITY SAMPLES FROM THE WISCONSIN-AGE DYE 3 ICE CORE

Sample no.	Sample depth m	Grain-size mm	$V_{\max 1}$ km/s	$V_{\max 2}$ km/s	$V_{\min}$ km/s	$V(45)$ km/s	Angle ( $\theta$ ) degree	Angle ( $\phi$ ) degree
63	1920.37	1.3	3.952	3.879	3.744	3.761	10	100
64	1923.29	1.6	3.931	3.858	3.755	3.777	5	99
65	1925.89	1.7	3.935	3.828	3.761	3.759	5	93
66	1927.37	1.5	3.934	3.860	3.790	3.790	5	100
67	1929.44	1.5	3.930	3.858	3.790	3.794	5	101
68	1931.34	0.87	3.897	3.860	3.755	3.771	10	98
69	1933.34	1.2	3.936	3.847	3.746	3.764	5	96
70	1936.84	1.3	3.941	3.853	3.753	3.783	15	104
71	1937.34	1.5	3.885	3.849	3.746	3.762	10	90
72	1940.28	1.7	3.950	3.873	3.765	3.782	10	100
73	1943.23	1.7	3.908	3.872	3.771	3.804	15	96
74	1943.31	1.4	3.863	3.827	3.758	3.769	12.5	91
75	1944.31	1.6	3.970	3.860	3.791	3.789	7.5	99
76	1947.31	1.6	3.978	3.870	3.769	3.769	5	98
77	1950.57	1.1	3.979	3.871	3.770	3.769	2.5	100
78	1952.31	0.81	3.919	3.846	3.743	3.743	5	96
79	1955.33	0.85	3.943	3.868	3.763	3.764	7.5	96
80	1957.31	1.3	3.972	3.879	3.775	3.775	0	101
81	1959.31	0.77	3.923	3.853	3.720	3.769	10	98
82	1962.31	1.1	3.919	3.866	3.765	3.783	15	94
83	1964.26	0.89	3.955	3.845	3.792	3.824	22.5	90
84	1966.46	0.88	3.921	3.850	3.749	3.749	5	95
85	1968.26	1.4	3.961	3.856	3.789	3.824	17.5	109
86	1971.26	2.0	3.992	3.882	3.747	3.779	7.5	104
87	1973.26	1.9	3.944	3.873	3.790	3.806	10	103
88	1975.26	1.9	3.997	3.891	3.789	3.804	12.5	103
89	1977.26	2.3	3.983	3.877	3.777	3.777	7.5	101
90	1979.26	1.7	3.963	3.869	3.763	3.782	10	103
91	1982.26	1.5	3.945	3.876	3.746	3.778	10	99
92	1985.26	2.2	3.957	3.849	3.780	3.779	2.5	99
93	1988.26	2.4	3.963	3.854	3.786	3.786	2.5	100
94	1991.26	1.7	3.988	3.882	3.783	3.799	10	103
95	1993.26	1.6	3.982	3.874	3.790	3.789	5	100
96	1995.18	2.9	3.948	3.877	3.809	3.834	12.5	108
97	1996.57	1.9	3.978	3.869	3.767	3.767	5	99
98	1999.18	2.3	3.955	3.882	3.778	3.804	5	99
99	1999.26	1.6	3.956	3.868	3.784	3.817	20	105
100	2002.26	2.6	4.000	3.860	3.761	3.768	2.5	106
101	2004.61	2.2	3.974	3.866	3.765	3.773	5	100
102	2006.05	2.2	3.979	3.874	3.743	3.766	2.5	111
103	2008.05	2.0	3.937	3.865	3.763	3.780	7.5	100
104	2010.05	2.0	3.992	3.863	3.793	3.794	0	105
105	2013.05	1.7	4.000	3.854	3.786	3.803	7.5	104
106	2015.07	1.2	3.959	3.853	3.785	3.784	5	103
107	2018.07	0.74	3.952	3.879	3.775	3.775	7.5	100
108	2020.07	0.74	3.955	3.848	3.749	3.772	12.5	101
109	2023.07	0.76	3.966	3.857	3.771	3.805	12.5	99
110	2025.95	0.82	3.959	3.853	3.720	3.779	15	109
111	2027.03	0.68	3.962	3.852	3.782	3.782	10	100
112	2029.44	0.74	3.958	3.849	3.763	3.779	2.5	99
113	2032.02	0.60	3.962	3.853	3.751	3.779	15	103
114	2034.00	0.45	3.911	3.839	3.771	3.789	7.5	101

Superimposed on the crystal-size data in Figure 5 are the  $\text{SO}_4^{2-}$  concentration levels for the same specimens (Langway and Goto-Azuma 1988, this volume).  $\text{SO}_4^{2-}$  concentration levels are found at higher and often more variable concentrations than either  $\text{Cl}^-$  or  $\text{NO}_3^-$ . In the Wisconsin age  $\text{SO}_4^{2-}$  ranges from about 20 to 210 ng/g;  $\text{Cl}^-$

ranges from about 20 to 100 ng/g and  $\text{NO}_3^-$  ranges from about 25 to 80 ng/g. In general the curves for  $\text{SO}_4^{2-}$  and  $\text{Cl}^-$  are coherent, increasing and decreasing in unison on a long-term basis. On the other hand, the  $\text{NO}_3^-$  concentration levels vary in low frequency with the other two species over the long-term.

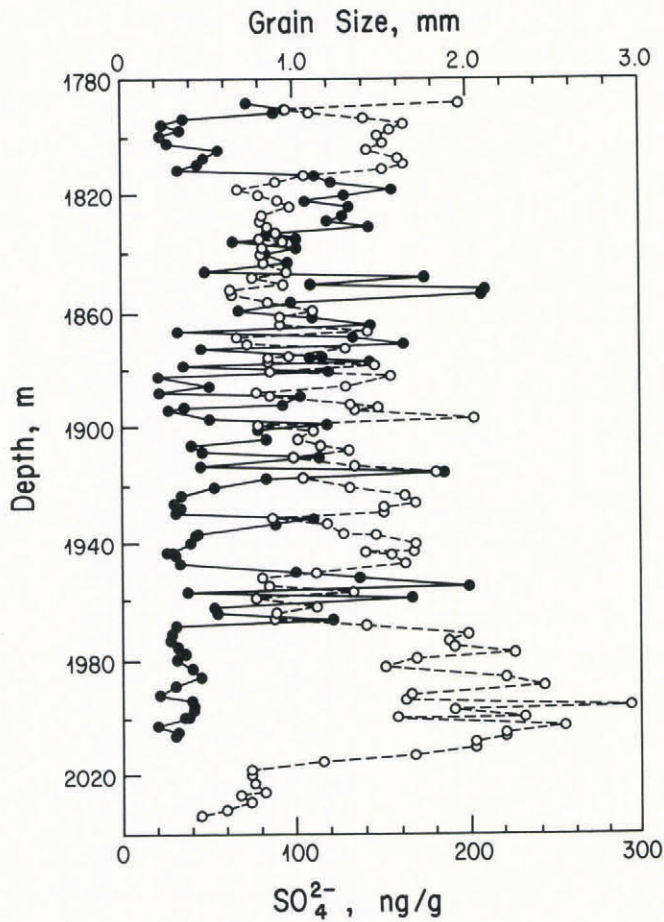


Fig.5. Crystal size and  $\text{SO}_4^{2-}$  concentration levels in Wisconsin-age ice. Crystal size is shown by open circles and  $\text{SO}_4^{2-}$  by solid circles.

#### DISCUSSIONS AND SUMMARY

For data interpretation it must be remembered that the original Dye 3 bore hole was augered with a  $6^\circ$  inclination from the true vertical (Gundestrup and Johnsen 1985). Since there was no azimuth control of the recovered core lengths, each value of  $\theta$  also includes a  $6^\circ$  true-direction uncertainty. Although  $\phi$  has not been converted into a tilt angle, it has the same directional uncertainty. A numerical measure of the variations in the concentration strengths of  $c$ -axes can be given by  $\delta V$ , the difference between  $V_{\max 2}$  and  $V_{\min}$  as obtained from the wave-velocity measurements.

$\text{SO}_4^{2-}$  has a multiple source origin and is usually the most prominent ionic species found in polar-ice deposits, often comprising 30% or more of the total soluble substances (Langway and Goto-Azuma 1988, this volume). For these reasons  $\text{SO}_4^{2-}$  was chosen as the most representative soluble impurity for examination in terms of the effects of impurities in the metamorphic processes governing changes in ice  $c$ -axes and crystal growth. The correlation between the  $c$ -axis fabric patterns and  $\text{SO}_4^{2-}$  content was investigated in detail. The results show that higher  $\text{SO}_4^{2-}$  content is always associated with higher  $\delta V$  (stronger  $c$ -axis concentration) and large  $\phi$  or smaller  $\theta$  values (less inclination of pole direction from the vertical core axis). On the other hand, wider variations are observed in  $\delta V$ ,  $\phi$  and  $\theta$  when the  $\text{SO}_4^{2-}$  content is low. A similar relationship was observed when correlating the  $\text{Cl}^-$  concentration levels. These findings suggest that a high concentration of chemical impurities may help to develop and strengthen the vertical preference of  $c$ -axis orientation patterns in the Wisconsin-age ice. Since all of the Wisconsin-age ice samples have strong single-maximum fabric patterns (including the low impurity-content samples), impurities alone cannot be the only parameter which controls the  $c$ -axis orientations.

A comparison of the crystal-size curve with the  $\text{SO}_4^{2-}$  concentration profile (Fig.5) clearly shows an inverse correlation. The smaller crystals are found at higher  $\text{SO}_4^{2-}$  concentration levels and, conversely, the larger crystals are found at low  $\text{SO}_4^{2-}$  concentration levels. A similar correlation is found with  $\text{Cl}^-$ . The size of an ice crystal is influenced by the rate of grain-boundary migration and/or recrystallization. It is well known in metallurgy that average crystal size increases over time, to lower the free energy of the ice crystals by minimizing the total grain-boundary area. This process takes place in the form of grain-boundary migration. Chemical impurities at grain boundaries cause grain-boundary migration to be retarded, resulting in a relative reduction in crystal size. The process of recrystallization may also cause reductions in crystal size by the nucleation of more crystals in a unit mass of ice. The intragranular or intergranular locations of impurities may also serve as nucleation sites for recrystallization, by lowering the crystal-boundary energy of the nucleated crystals. Another cause for crystal-size reduction is the rearrangement of dislocations to form new crystal boundaries. These processes take place by plastic deformation, accompanied by dislocation multiplication processes which may be affected by the existence of impurities. Little is known about the exact roles of  $\text{SO}_4^{2-}$ ,  $\text{Cl}^-$  or other impurities in the above processes. Dust is another parameter which has an inverse correlation with crystal size (Hammer and others 1985). It is clear that a strong positive cross-correlation exists between  $\text{SO}_4^{2-}$ ,  $\text{Cl}^-$  and dust and crystal size. However, more research is essential to explain the relative influences these species have on grain-size variation.

In summary, this investigation has shown by crystal-size and  $c$ -axis measurements that no changes have occurred in these parameters during the period of more than 5 years since the Dye 3 ice core was recovered. A new multi-directional ultrasonic wave-velocity measurement technique provides an accurate and relatively rapid method of obtaining mean  $c$ -axis orientation patterns from ice cores. Results of the 22 new thin-section analyses on the Wisconsin-age ice indicate that strong single-maximum fabric patterns exist at all levels measured. The results of the 114 ultrasonically measured specimens confirm the uniformly strong elastic anisotropy in Wisconsin-age ice, and in the bottom 29 m of silty ice, due to the strongly preferred, near-vertical,  $c$ -axis orientations. Crystal sizes range between 0.5 and 3.0 mm. Smaller-size crystals are found at high impurity concentrations and, conversely, larger crystals are found at low impurity concentrations. These multiple-study results indicate that crystal size is influenced by impurity content but that impurity concentration levels have less of an effect on the formation of orientation patterns.

#### ACKNOWLEDGEMENTS

This work was supported by the U.S. National Science Foundation (DPP grant no. 8520911). The Department of Applied Physics, Hokkaido University, Japan, made possible the visit of N. Azuma to the State University of New York at Buffalo for two months in 1984 to conduct the manual thin-section analyses. The chemical measurements were made by Carol Clemency and Dr K Goto-Azuma.

#### REFERENCES

- Azuma N Unpublished Experimental studies on the development of texture and the flow behavior of ice in polar ice sheets. (PhD thesis, Hokkaido University, 1986)
- Bennett H F 1972 Measurements of ultrasonic wave velocities in ice cores from Greenland and Antarctica. *CRREL Research Report 237*
- Dansgaard W and 6 others 1982 A new Greenland deep ice core. *Science* 218(4579): 1273-1277
- Dansgaard W, Clausen H B, Gundestrup N, Johnsen S J, Rygner C 1985 Dating and climatic interpretation of two deep Greenland ice cores. In Langway C C Jr, Oeschger H, Dansgaard W (eds) *Greenland ice core: geophysics, geochemistry and the environment*. Washington, DC, American Geophysical Union: 71-76 (Geophysical Monograph 33)

- Gundestrup N S, Johnsen S J 1985 A battery powered, instrumented deep ice core drill for liquid filled holes. In Langway C C Jr, Oeschger H, Dansgaard W (eds) *Greenland ice core: geophysics, geochemistry and the environment*. Washington, DC, American Geophysical Union: 19-22 (Geophysical Monograph 33)
- Hammer C U, Clausen H B, Dansgaard W, Neftel A, Kristinsdottir P, Johnson E 1985 Continuous impurity analysis along the Dye 3 deep core. In Langway C C Jr, Oeschger H, Dansgaard W (eds) *Greenland ice core: geophysics, geochemistry and the environment*. Washington, DC, American Geophysical Union: 90-94 (Geophysical Monograph 33)
- Herron M M, Langway C C Jr 1985 Chloride, nitrate, and sulfate in the Dye 3 and Camp Century, Greenland ice cores. In Langway C C Jr, Oeschger H, Dansgaard W (eds) *Greenland ice core: geophysics, geochemistry and the environment*. Washington, DC, American Geophysical Union: 77-84 (Geophysical Monograph 33)
- Herron S L, Langway C C Jr, Brugger K A 1985 Ultrasonic velocities and crystalline anisotropy in the ice core from Dye 3, Greenland. In Langway C C Jr, Oeschger H, Dansgaard W (eds) *Greenland ice core: geophysics, geochemistry and the environment*. Washington, DC, American Geophysical Union: 23-31 (Geophysical Monograph 33)
- Kohnen H, Bentley C R 1977 Ultrasonic measurements on ice cores from Ross Ice Shelf, Antarctica, drill hole. *Antarctic Journal of the United States* 12(4): 148-150
- Kohnen H, Langway C C Jr 1977 Untersuchungen mit Ultraschall an Eisbohrkernen aus Zentralgrönland. *Polarforschung* 47(1/2): 1-10
- Langway C C Jr 1958 Ice fabrics and the universal stage. *US Army Snow, Ice and Permafrost Research Establishment. Technical Report* 62
- Langway C C Jr, Goto-Azuma K 1988 Temporal variations in the deep ice core chemistry record from Dye 3, Greenland. *Annals of Glaciology* 10: 209
- Langway C C Jr, Oeschger H, Dansgaard W 1985 The Greenland Ice Sheet Program in perspective. In Langway C C Jr, Oeschger H, Dansgaard W (eds) *Greenland ice core: geophysics, geochemistry and the environment*. Washington, DC, American Geophysical Union: 1-8 (Geophysical Monograph 33)
- Shoji H, Langway C C Jr 1982 Air hydrate inclusions in fresh ice core. *Nature* 298(5874): 548-550
- Shoji H, Langway C C Jr 1983 Volume relaxation of air inclusions in a fresh ice core. *Journal of Physical Chemistry* 87(21): 4111-4114
- Shoji H, Langway C C Jr 1985 The ice flow velocity profile for Dye-3, Greenland. *Geophysical Research Letters* 12(12): 797-800